Performance Comparison of Two-, Three- and Four-coil E-Textile Wireless Power Transfer Systems

Yixuan Sun, Sheng Yong, Nicholas Harris and Stephen Beeby, *Fellow, IEEE*

***Abstract*—Magnetically coupled resonant wireless power transfer (MR-WPT) can efficiently power e-textile systems. Different coil configurations (2, 3 and 4-coil structures) were investigated using planar textile coils of size 14.5 x 15 cm fabricated on cotton substrates using an embroidery process whereby silk-coated copper Litz wire forms the conductive track. For each configuration, the efficiency of the MR-WPT has been explored at different separation distances, misalignments and when subject to bending. The results show that the 2-coil structure was the most efficient at short distances (below 10 cm). However, the 4-coil system has the best performance at distances over 11 cm and when subject to axial misalignment, variations in coil orientation and when the coils are deformed by bending. The planar 4-coil configuration is therefore recommended for use in most practical applications. The coils were wash tested, and whilst they continue to function up to 15 wash cycles, performance does deteriorate due to a change in the coil properties. The coils can withstand 1000 bending cycles but there is a drop in performance of 43% in power transfer efficiency due to increasing coil resistance. Performance over longer separation distances is limited due to the properties of textile coils.**

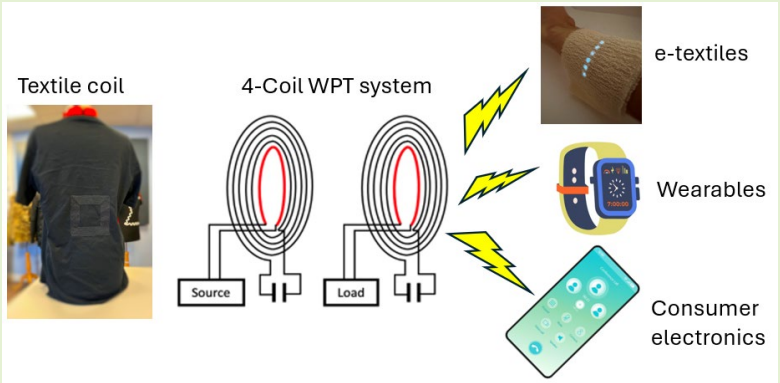

***Index Terms*— Embroidered coil, magnetic resonant coupling, textile coil, wearable coil, wireless charging, wireless power transfer (WPT)**

I. Introduction

TODAY, wearable electronics attract broad interest as a platform for portable personal electronic devices for use in, for example, health monitoring and fitness tracking. One form of wearable technology is electronic textiles (e-textiles) where sensors and associated processing and communication electronics are embedded within a fabric [1] enabling the monitoring of, for example, the user's bio signals [2] or their environment [3]. One key obstacle to e-textiles technology is the reliance on conventional rigid batteries to supply power. Batteries are incompatible with the properties and feel of a textile, are bulky and intrusive and must be removed for machine washing. The nature of e-textiles requires a power supply to be flexible, unobtrusive and able to survive the rigors of use. Amongst the various options for energy harvesting-based power supplies [4], textile-compatible wireless power transfer (WPT) using RF [5] – [8] or inductive approaches [9] – [11] offers a potentially convenient solution. Textile-based electromagnetic WPT offers the potential for efficient transmission of relatively high-power levels >1W in the near-field [12] using magnetically coupled source and receiver coils. In future applications, WPT could be used to recharge textile-based energy storage (e.g. textile supercapacitors [13] or batteries [14]) that store the energy ready for use as required. An example scenario has the transmitter placed inside a drawer or wardrobe, and the garments with the receiver and energy storage can be recharged wirelessly simply by placing them inside the drawer/wardrobe. However, the constraints imposed by the fabrication of a flexible textile coil restrict the coil properties, ultimately limiting the quality factor (Q) effecting WPT performance.

Inductive near-field WPT is an established and well understood technology. Conventional inductive wireless power transfer uses near-field magnetic induction between the primary and secondary coils [15]. The transferred power is attenuated according to the cube of reciprocal of the distance, resulting in a limited transmission distance. Power transfer efficiency and

This work of Stephen Beeby was supported by the U.K. Royal Academy of Engineering under the Chairs in Emerging Technologies Scheme. The authors are with The Centre for Flexible Electronics and E-Textiles, School of Electronics and Computer Science, University of Southampton, Southampton, SO17 1BJ, UK. (e-mail: spb@soton.ac.uk).

range can be increased by operating at resonance [16]. Conventional two-coil magnetically coupled resonant WPT (MR-WPT) is most efficient over transmission distances smaller than the diameter of the coupled coils [17][18]. In 2007, a research group from MIT proposed a strongly coupled magnetic resonance (SCMR) method based on a four-coil design (source coil, transmitting coil, receiving coil, and load coil) capable of transmitting 60 watts with 40% efficiency at 2.4 m transfer distance [19]. This study demonstrated efficient power transfer over distances up to 2 m (8 times the coil radius of 25 cm). Rather than being directly connected to the power source and load, the two resonant transmission coils were inductively coupled with separate source and load coils, which are connected to the power source or load. Other studies [20] - [23] have also demonstrated the benefits of the SCMR configuration. Three-coil systems, where a single additional coil acts as either a source or load coil from the conventional four-coil system, have also demonstrated high efficiency and strong coupling at mid-range distances [24]. When the additional coil is used as the source coil, the input impedance is increased, reducing the current and power drawn from the input signal and increasing energy efficiency [25][26]. When the additional coil is placed as a load coil, the load impedance can be adjusted to deliver more power to the load, improving power efficiency [17][24].

Studies have shown that efficiency changes depending upon the coupling between the source/load coils and the transmitting coils [27]. This can result in the efficiency of the four-coil SMCR system decreasing as the gap between transmitting coils reduces below a given transfer distance threshold [28]. Below this threshold separation distance (or critical coupling point), the optimum resonant frequency splits, and maximum efficiency occurs at two distinct frequencies, one above and one below the original resonant frequency. Frequency splitting depends upon the source resistance and coupling between source/load coils and the transmitting coils [28] and is discussed further in section II. Conformal SCMR (CSCMR) has the single-loop source and load coils coplanar (i.e. on the same plane) with resonant coils (Fig. 1), requiring less volume than conventional SCMR systems [29][30]. This configuration is more relevant for textile-based systems where coils are implemented on a single fabric layer. Textile coil fabrication methods result in higher coil resistances and lower Q-factors, which reduce WPT efficiency compared with other coil types. Conformal textile transmitters and receivers realized using embroidered conductive textile threads and by cutting out conductive textiles into the required shape [31][32] demonstrate a lower transmission efficiency than for the printed circuit board (PCB) equivalent. Other methods used to fabricate textile coils include printed silver coils (efficiency 1.2% [33]) and embroidered composite yarns (efficiency 46.2% [10]). An experimental evaluation of printed, embroidered and couched Litz wire textile coils has been presented by Grabham et al. [34]. Couching is an automated embroidery process whereby the Litz wire is attached to the surface of the base fabric with small stitches of normal thread. The Litz wire achieved the lowest coil resistance, the highest end-to-end DC-DC efficiency and had the least effect on the feel of the textile [34].

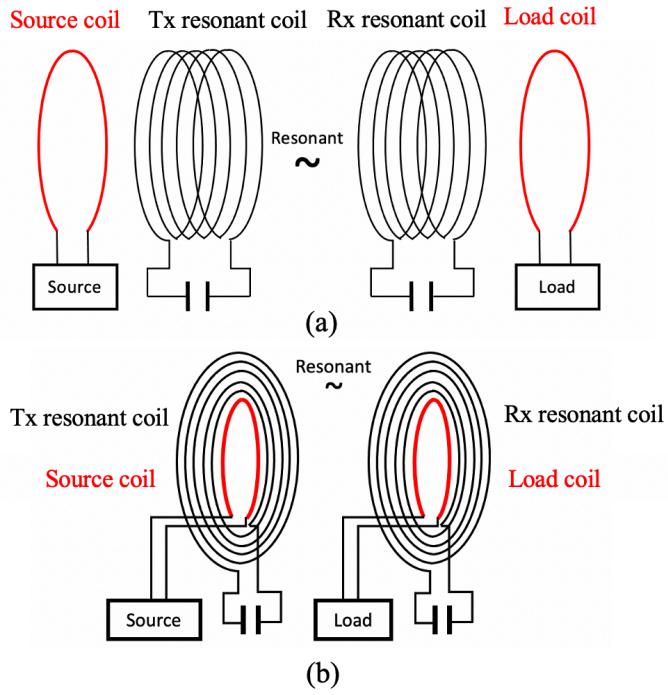

Fig. 1. Schematic of (a) the conventional four-coil MR-WPT and (b) the typical conformal planar four-coil MR-WPT.

Whilst 2-, 3-, and 4-coil WPT systems have been well studied, the novelty presented here is the comparative evaluation of these systems using conformal textile transmitters and receivers. A few studies have investigated wearable resonant WPT systems using 2, 3 and 4-coil configurations [10][11][25][35] - [37]. Heo et al. [10] presented a planar spiral four-coil MR-WPT using couched Litz coils fabricated on a cotton substrate. This work highlighted the importance of wire resistivity on the Q-factor and efficiency. The wearable three-coil structured resonant WPT was demonstrated in [11] with 6 cm x 6 cm coils fabricated by couched Litz wire on a polyester/cotton substrate achieved 82% efficiency at a transfer distance <1 cm.

This paper presents the first comprehensive comparative experimental investigation of two-dimensional planar textile 2-coil, 3-coil, and 4-coil MR-WPT systems using the previously identified optimum fabrication process (couched Litz wires). Replicating typical use case scenarios, the impact of the typically inferior textile coil properties on the transmission efficiency of each system has been studied over varying transmission distances, for different orientations and alignments of the coils and under the effects of bending. The ability of the different WPT systems to recharge a capacitor and a mobile phone is demonstrated, demonstrating their ability to recharge consumer electronic devices. Finally, a comprehensive evaluation of the effects of multiple machine wash cycles on the textile coils is presented.

II. Design And Experimental Setup

The proposed models are shown in Fig. 2, with the coils denoted L_1 to L_4. All coils were designed in a planar square

spiral shape. The 2-coil and 4-coil MR-WPT systems had identical symmetric transmitting (Tx) and receiving coils (Rx). In the 4-coil design, the resonant coils were enclosed by a single-turn driving and load coil (L_1 and L_4). For the 3-coil system, the additional coil was used as the source coil.

The transmitting and receiving coils are designed to be identical (L_2=L_3). The systems can operate at the same resonant frequency (1) by adding lumped capacitors:

$$f = \frac{1}{2\pi\sqrt{L_2C_1}} = \frac{1}{2\pi\sqrt{L_3C_2}} \quad (1)$$

The lumped capacitance of the transmitting and receiving coils can be calculated using (2), although consideration should also be given to the parasitic capacitance of the coil:

$$C = \frac{1}{4\pi^2 f^2 L} \quad (2)$$

Equation 2 predicts an ideal tuning capacitance of 29 pF, however, in practice, the tuning capacitance was between 27 and 28 pF depending upon the parasitic capacitance of the coil. Power is transferred by the coupling between all coils, and the transfer efficiency can be determined as a function of the mutual inductance M, which is defined as the ratio of the voltage induced in inductor j to the rate of change of current in inductor i [17]. Reciprocity implies that $M_{ij} = M_{ji}$. The mutual inductance M_{ij} between coils can be determined by geometric parameters and coil separation. To calculate the mutual inductance between two multi-turn coils, each turn of the coils is considered as one filament to compute the sum of mutual inductance M_{ij} for each turn with the aid of Neumann's equation [22]. The mutual inductance M between two concentric planar coils with N turns can be represented in (3) as a combination of M_{ij}. The parameter ρ is determined by the shape of coils. For circular or rectangular coils, ρ is 1 or $(4/\pi)^2$[22].

$$M = \rho \times \Sigma_{i=1}^{i=N}\Sigma_{j=1}^{j=N} M_{ij} \quad (3)$$

$$M_{ij} = k_{ij}\sqrt{L_iL_j} \quad (4)$$

It has been shown that the rectangular shape is better for planar coil design [38][39] due to the larger inductive area compared to the circular shape of the same size. Therefore, the self-inductance and mutual inductance become higher, the coupling between coils is enhanced, and the tolerance to coil misalignments is improved. The spacing between each coil turn is another key factor when designing the coils. The self- and mutual inductance of the coils increases with decreasing gap between coil turns [39].

M_{ij} can be represented by coupling coefficient k_{ij} by (4). Therefore, the mutual inductance between L_2 and L_3 is derived as $M_{23} = k_{23}\sqrt{L_2L_3}$. At critical coupling, where $k = k_c$, the WPT systems have a maximum transfer efficiency. The mutual inductance M_{23} increases as the gap between coils reduces, where $k > k_c$. The transfer efficiency decreases due to the reduced input impedance and increased input impedance angle [28][40]. The input impedance angle, representing the phase shift between voltage and current at the source, becomes significant at close gaps, reducing the transferred power between the source and source coil. Moreover, the decrease in input impedance results in an increased source current and more losses at the source. Below and above the resonant frequency, the impact of the two factors that cause the reduction in efficiency becomes smaller, the transfer efficiency increases gradually to peak at two frequencies [28]. This is the frequency splitting phenomenon, where the coils are operating in the over-coupled region.

Wireless power transfer efficiency η can be obtained using the two-port circuit analysis. Equation (5) shows its relationship with the transmission coefficient S_{21} [17][20][40] where P_{in} is the AC input power and P_{out} the AC output power.

$$\eta = \frac{P_{out}}{P_{in}} = |S_{21}|^2 \quad (5)$$

An automated sewing machine PFAFF Creative 3.0 was used to couch the conductive Litz wire onto a cotton fabric ($\varepsilon_r = 2.1$), thickness 0.2 mm. The stitching thread was polyester with a stitch tension of 4.4 to 5 (arbitrary units), the stitch speed was 150 stitches/minute and the stitch length was 1 mm which is the smallest length available. Higher stitch tension pulls the Litz wire into the fabric and causes bunching of the fabric around the embroidery stitches which distorts the coil geometry. Conversely, lower tension will fail to properly secure the wire, resulting in a loose and imprecise coil geometry. The silk-coated copper Litz wire consists of 36 individual strands of 40 µm enamelled copper wire and has a conductivity of 0.065 Ω/m. The wire is insulated by the enamel and silk coating to enable the coil ends to cross over the coil turns without short-circuiting the coil. The couched coils are shown in Fig. 3. The resonant (Tx and Rx) coils are square-shaped with 14.5 x 15 cm side lengths, 10 turns with a 4 mm separation between turns.

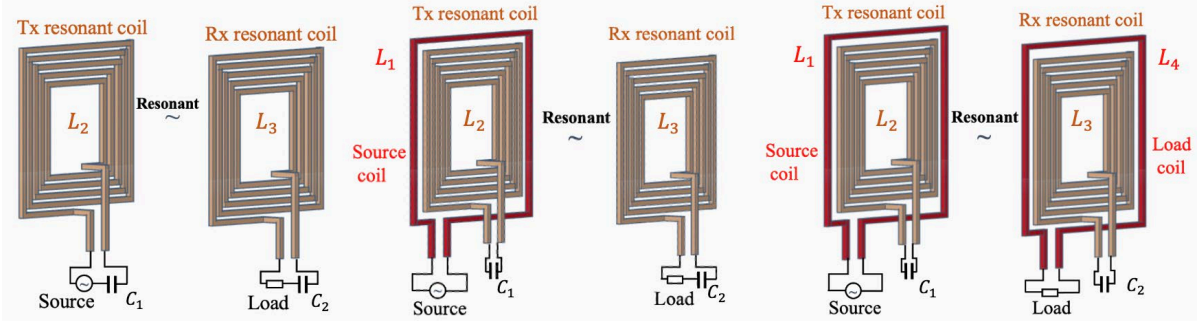

Fig. 2. The schematic of proposed planar MR-WPT systems. (a) The two-coil MR-WPT. (b) The three-coil MR-WPT. (c) The four-coil MR-WPT.

The square single-turn coupling coils (driving and load) are located 4 mm away from the outermost turn of the resonant coils. The typical inductance and resistance of the Tx and Rx coils are around 18.9 μH and 10.6 Ohms, leading to a q-factor (from equation 6) of 74 at the target resonant frequency is 6.78 MHz.

$$Q = \omega \frac{L}{R} \tag{6}$$

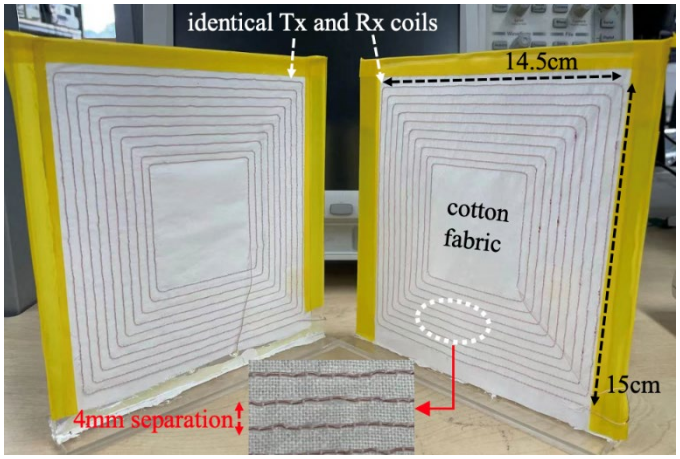

Fig. 3. Photograph of the planar transmitter and receiver coils used in the two-coil MR-WPT configuration.

The characteristics of all fabricated coils were measured using a WK 6500B impedance analyzer at this frequency and the value of the resonant tuning capacitors was determined using equation (3). For testing, the cotton fabric was attached to acrylic supports, enabling the relative position and form of the coils to be precisely controlled to ensure accurate and repeatable measurements.

The MR-WPT performance was analyzed by measuring PTE using two approaches. The first approach is to use the two-port vector network analyzer (VNA) to evaluate the scattering parameter S_{21} of the WPT system. The second approach utilizes a 50 Ω power generator transferring a steady input 20 dBm P_{in}. Meanwhile, the output voltage across the load is measured by an oscilloscope to determine the output power $P_{out} = V^2/R$. In both cases, the PTE is calculated using equation (5).

III. Experiments And Results

The S_{21} coefficient versus frequency and PTE at resonance at 6.78 MHz has been studied for the 2, 3 and 4-coil systems under varying Tx and Rx coil separation distances. PTE has also been determined for different Rx orientation angles, axial misalignments, and under bending.

A. Transfer Distance

Various separation distances between the Tx and Rx coils (5, 10, 15, and 20 cm) were investigated with the VNA transmitting 0 dBm power from 1 to 20 MHz. The forward power transmission is plotted against frequency in Fig. 4. The highest PTE can be found at the frequency where the S_{21} coefficient reaches its peak. At 5 cm separation, two peaks were observed from the S_{21} plot (Fig. 4a) with the first peak located at around 6.2 MHz and the second near 7.6 MHz. This is the frequency splitting phenomenon as discussed in the previous section. At 6.2 MHz, S_{21} was around -1 dB, showing that most power was transferred to port 2. The magnitude of S_{21} at the target 6.78 MHz resonant frequency was -4.77 dB, -5.74 dB and -7.61 dB for the 2, 3 and 4-coil systems respectively. Results for a separation distance of 10 cm (Fig. 4b) indicate the onset of frequency splitting with an S_{21} at 6.78 MHz of -1.34 dB. More power can be transferred from the transmitter to the receiver at a greater distance due to the reduction in frequency splitting. When the separation increased to 15 cm (Fig. 4c), the frequency splitting disappeared for all systems. The S_{21} at 6.78 MHz was -7.25 dB, -4.28 dB and -3.04 dB for the 2, 3 and 4-coil systems respectively. The resonant coupling of coils became significantly lower at a separation distance of 20 cm (Fig. 4d) with around half the power being received compared with 15 cm. For both 15 and 20 cm separations, the 2-coil system transfers the least power and the 4-coil system is most effective.

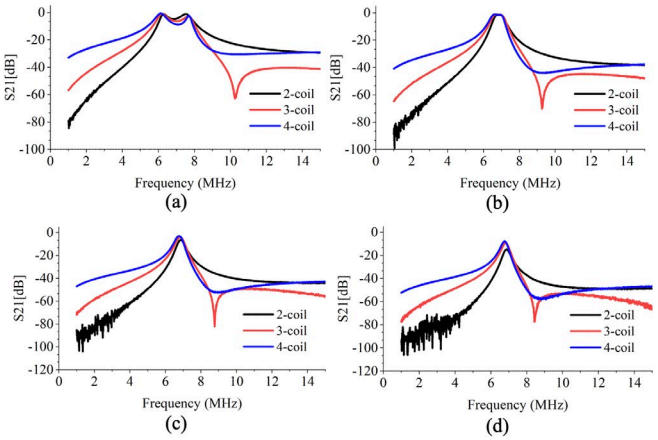

Fig. 4. S_{21} of the 2-coil, 3-coil and 4-coil MR-WPTs when the coil separation is (a) 5 cm, (b) 10 cm, (c) 15 cm, and (d) 20 cm.

The PTE of each system was studied versus transfer distances from 4 cm to 25 cm using both the VNA and oscilloscope-based measurement. Fig. 5a shows the plots of RMS output voltage across the load versus transfer distance. The maximum voltage for the 2, 3 and 4-coil systems was 2.01 V at 9 cm, 2.04 V at 10 cm, and 1.9 V at 11 cm, respectively. These correspond to the separation distances at which peak PTE occurs and are the critical coupling point for each system. Systems enter the over-coupled region at a separation distance below these values, and the output voltage falls due to the increased source current and greater losses at the source. The corresponding maximum power delivered to the load was 81 mW, 83 mW for the 3-coil and 72 mW for the 2, 3 and 4-coil systems, respectively. As the transfer distance increases beyond the critical coupling point, the 3-coil and 4-coil systems showed a comparable and higher power delivery to the load than the 2-coil system.

Fig. 5b shows the PTE, which matches the RMS voltage results. The peak efficiency of the systems at the critical coupling point from the VNA measurements was 77.98% at 9 cm (2-coil), 77.45% at 10 cm (3-coil), and 75.16% at 11 cm (4-coil). The PTE falls in the over- and under-coupled regions, with the 4-coil system achieving the highest PTE at separation

distances above 11 cm. The results are typical for the 2, 3 and 4-coil systems [18][41]. However, even for the 4-coil system, the PTE falls away sharply after the critical coupling point and is at around 50% at a separation distance equal to the coil diameter. This is a consequence of the relatively low q-factors of the textile coils. A comparison of the efficiency vs transfer distance between this work and other textile-based MR-WPT systems is shown in table 1. This work achieves higher efficiencies at longer transfer distances than previous works.

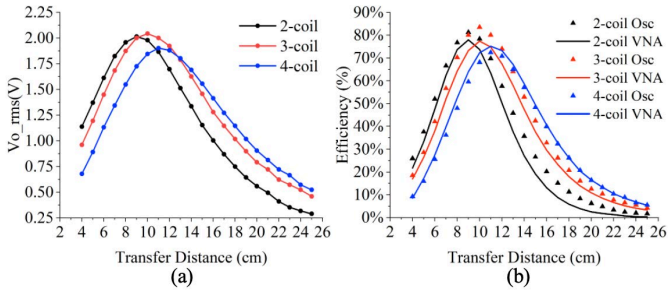

Fig. 5. The outputs of 2-coil, 3-coil and 4-coil MR-WPTs plotted against transfer distance at 6.78 MHz. (a) The output RMS voltage across the 50Ω load.(b) The power transfer efficiency.

When operating in the over-coupled region, the two characteristic peaks in S_{21} (Fig. 4a) can be denoted as the odd mode (peak at the lower frequency) and even mode (higher frequency peak) [40]. The peak frequency (the frequency at which S_{21} reaches its maximum) of each mode domain was measured for versus separation distances from 4 cm (Fig. 6a). As the separation distance increases from 4 cm, the peak mode frequencies converge at the critical coupling point and at the target frequency of 6.78 MHz. The transfer efficiencies of the systems operating in the odd and even modes were studied versus separation distance, with the frequency varied to track the peaks. The PTE of the odd mode (Fig. 6b) remains fairly constant for all coil systems across the over-coupled region, and the 4-coil system demonstrates the highest PTE at distances less than 8 cm. In contrast, in the even mode (Fig. 6c), the 2-coil system maintains the highest PTE throughout the over-coupled region, whilst the 3 and 4-coil systems show a sharp drop-off. Overall, when operated in the over-coupled region, efficiencies were improved for all systems when the frequency was tuned to the odd mode, which is consistent with other findings [40][42].

B. Axial and Orientation Misalignment

The experiment to explore the impact of axial misalignment is shown in Fig. 7a with the Rx coil maintained at a fixed 15 cm separation distance and aligned in parallel with the Tx coil. Fig. 7b shows the comparison of the PTE of the 2, 3 and 4-coil systems as the axial misalignment distance was increased from 0 cm (aligned) to 18 cm (over twice the coil radius). The PTE falls with increasing axial misalignment, with the efficiency being 50 % lower at a misalignment distance of 8 cm. The efficiency decreases to zero at 18 cm misalignment for all configurations, meaning the Tx and Rx coils are fully uncoupled at this point. The results agreed with similar studies [30][43]. Liu *et al.* demonstrated that the CSCMR had less sensitivity to misalignment than conventional SCMR due to its planar configuration [30]. The rigid copper loops achieved around 18% PTE at an axial displacement equal to the diameter of the loop [30]. In comparison, the textile coils in this study mean the PTE is just 5% for the 4-coil systems when axially displaced by the coil diameter.

Orientation misalignment was explored by rotating the Rx coils from 0 degrees (parallel) to 90 degrees (perpendicular, Fig. 7c) to the Tx coil at a fixed separation distance of 15 cm. Fig. 7d shows the PTE against orientation angle which shows an increasing rate of reduction as the angle increases. As the Rx coil was rotated, the magnetic flux intersecting the coil decreased, leading to a reduction in the mutual coupling. The angular misalignment results show good agreement with COMSOL model of angularly displaced 2D planar systems [44]. In both axial and orientation misalignment cases, the 4-coil system shows the greatest tolerance and is far superior to the 2-coil textile system.

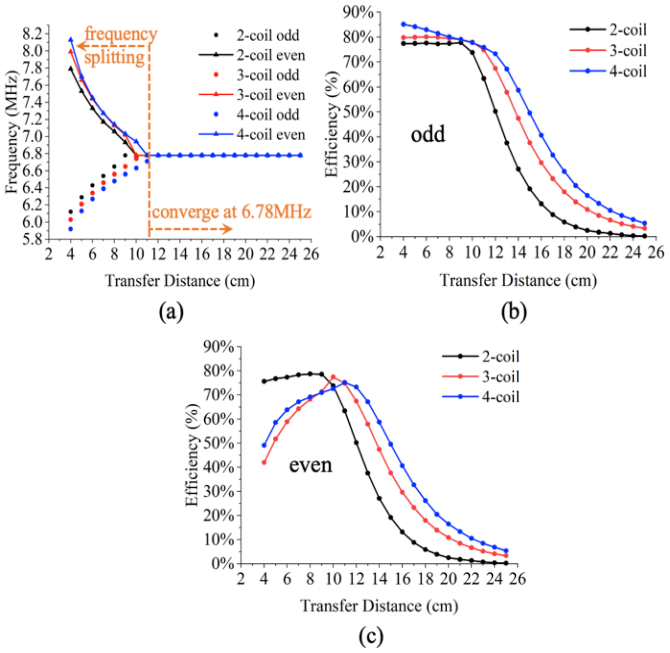

Fig. 6. (a) The frequency at two modes varied with transfer distance for 2-coil, 3-coil and 4-coil MR-WPTs. The power transfer efficiency of 2-coil, 3-coil and 4-coil MR-WPTs plotted against transfer distance at (b) odd mode and (c) even mode.

C. Bending Study

In flexible textile applications, the coils will likely bend with the flex and drape of the fabric during use. The Rx coil was bent into an arc over a plastic support used to define the bending radius. When the coil is flat the bending is 0 degrees, and when the coil is bent into a full semicircle, the bending is 180 degrees (see Fig. 8a). Fig. 8b shows the experimental setup used to explore the effect of bending the textile coils. The experiments were performed with the separation distance fixed at 15 cm, and the results are shown in Fig. 8c.

TABLE 1
A COMPARISON OF TRANSFER EFFICIENCY VS TRANSFER DISTANCE BETWEEN THIS WORK AND OTHER TEXTILE-BASED MR-WPT SYSTEMS

Author/ Year	Coupling Type	Coil Diameter D or Length (cm)	Fabrication and material	Substrate	Frequency (MHz)	Max. PTE at distance	Effective transmission range (cm) at 50% PTE	Normalised range (effective range / Rx size)
This work	MR 2-coil, 3-coil, 4-coil Rectangle	Tx & Rx: 14.5×15	Embroidered Litz wires	Cotton	6.78	2-coil: 73.5% at 9 cm 3-coil: 77.5% at 10 cm 4-coil: 75.2% at 11 cm	2-coil: 12 (50.2%) 3-coil: 14 (47.4%) 4-coil: 15 (49.7%)	2-coil: 0.8 3-coil: 0.93 4-coil: 1
M. J. Jeong et al. 2016 [37]	MR 4-coil Helical, circular	Tx: 12 Rx: 14	Couched, Ag coated copper wire wrapped around a polyester yarn	Non-woven polyester fabric	14.5	50% at 6.5 cm	6.5	0.46
S. H. Kang et al. 2016 [42]	MR 4-coil Planar, Circle	Tx & Rx: 12	Bonded Cu tape Painted Ag paste	Polyester	Cu: 6.44 Ag: 5.9	Cu: 55.6% at 5 cm Ag: 3.8% at 1 cm	5 (Cu)	0.42 (Cu)
E. Heo et al. 2018 [10]	MR 4-coil Planar, Rectangle	Tx: 30×30 Rx: 8×12	Embroidered Tx: Cu Litz wire Rx: Ag thread	Tx: PTFE Rx: Cotton	6.78	42.6% at 5 cm	5	0.11
M. Wagih et al. 2020 [11]	MR 3-coil (dual Rx) Planar, Rectangle	Tx: 4.6×4 Rx: 6×6	Couched Cu Litz wires	Polyester -cotton	6.78	90% at 2.2 cm	5	0.83
M. Wagih et al. 2024 [12]	MR 2-coil Planar, Rectangle	Tx & Rx: D=15	Screen-printed Ag	75 µm thick PU film laminated on textile	6.78	67% at <0.5 cm	<0.5	0.03

It was observed that the PTE dropped linearly for the 2-coil system, very close to linear for the 3-coil system and is least linear for the 4-coil. The 4-coil system is initially less sensitive to bending angle but shows a sharper decrease in efficiency when the bending angle increases beyond 90 degrees.

D. Wash Testing

For textile coils used in wearable, garment-based applications, the ability to withstand machine washing is an important indicator of robustness and practicality. Machine washing is a physically harsh environment that will affect coil geometry, operating characteristics, functionality and appearance over time. The power transfer performance was evaluated for the 2-coil system at 6.78 MHz after a specified number of wash cycles, primarily by monitoring the power efficiency over distance. The influence of the automated embroidered couching process parameters sewing tension (embroidery machine stitching tension) and presence of stiffener (non-woven interfacing polyester support that is typically removed after stitching) on coil durability was also investigated.

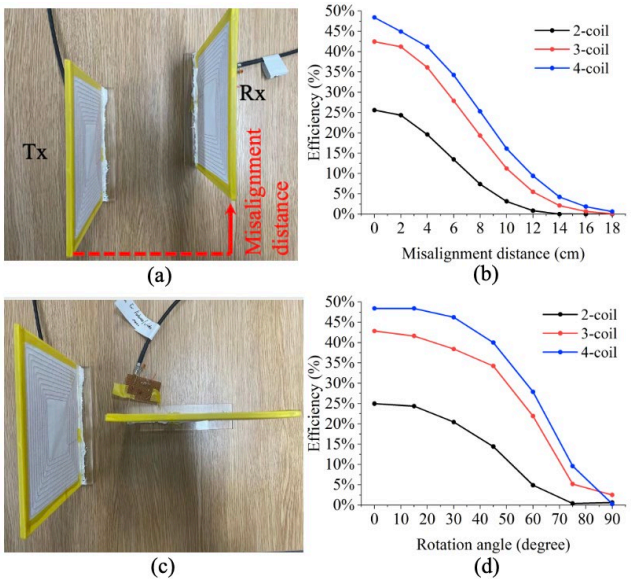

Fig. 7. (a) The model of coils axial misalignments. (b) Rx coils axial misaligned at 15cm separation. (c) Rx coil was rotated at 90 degrees. (d) The power transfer efficiency for Rx coils rotated at 15 cm separation.

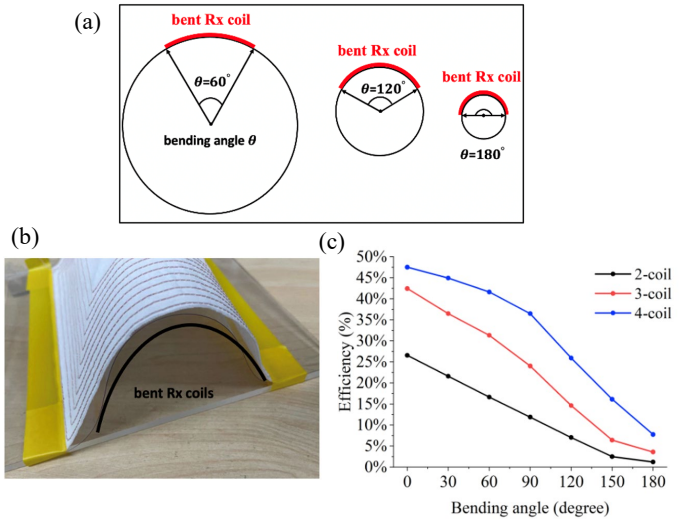

Fig. 8. (a) The Rx coil is bent as into an arc. (b) Diagram illustrating the bending angles. (c) The power transfer efficiency for Rx coils rotated at 15cm separation.

Six t-shirt samples were assembled, each featuring identical square coils, 14 x 14.5 cm with 10 turns (Fig. 9), 25.6 µH, 8.72 Ohm, and a Q of 125. The t-shirts were washed together in a household washing machine (Becko WME7247W) operating on a 40-minute cycle, with 1000 rpm spin dry. In addition, one t-shirt was tumble-dried, and one t-shirt was placed in a laundry bag during washing. One coil was embroidered onto a separate 15 cm square piece of fabric (identical to the t-shirt fabric) that was then laminated onto a t-shirt using a hot melt adhesive film (thermoplastic polyurethane film, 100 µm thick) and a hot press at 190°C. This approach sandwiches the coil between two layers of fabric, potentially improving durability. The details of each t-shirt are given in Table 2.

In Fig. 11a, t-shirt sample 1 (coil couched with the original parameters used in the previous sections of the paper) showed a 50% reduction in power transfer efficiency from 74% to 38% after 9 washes with the separation distance fixed at 11 cm. The efficiency continued to fall with subsequent wash cycles, reaching around 10% after 15 washes. Of the remaining coils, the least affected by washing were samples 2 and 5, i.e., coils fabricated with increased stitching tension or washed in a laundry bag. In Fig. 11b, t-shirt sample 2 demonstrated a power transfer efficiency of 48.64% after 9 wash cycles and retained 26% after 15 washes. Fig. 11c shows that the efficiency of t-shirt sample 5 (placed in a laundry bag during washing) was 24.8% after 15 washes. After 9 washes, the laminated t-shirt, sample 6, had the lowest efficiency of 12%. This method of coil assembly did not provide additional protection and led to wires becoming exposed and the coil breaking after 11 washes, at which point it was removed from the study. T-shirt sample 3 (fabricated without the stiffener) showed the greatest deformation and achieved the lowest PTE of 5.28% after 15 washes. The results for the tumble-dried t-shirt sample 4 suggest tumble drying has little effect on coil performance compared to machine washing.

Fig. 9. Example coil on a t-shirt used in wash testing.

TABLE 2
TEXTILE COIL SAMPLES FOR WASH TESTING

No.	Tension	Stiffener	Drying	Laundry bag	Laminated
1	4.6	Yes	Air	No	No
2	5.6	Yes	Air	No	No
3	4.6	No	Air	No	No
4	4.6	Yes	Tumble	No	No
5	4.6	Yes	Air	Yes	No
6	4.6	Yes	Air	No	Yes

As observed in Fig. 11d, 11e and 11f, machine washing resulted in a reduction in the optimal transfer distance and a gradual decline in the efficiency for all t-shirt samples after each wash cycle. Mechanical stress from machine washing deformed the coils, thus changing the resonant frequency and reducing the Q-factor. For example, the Q-factor for the coil in sample 5 fell to 13 after 7 wash cycles.

E. Durability under Cyclical Bending

The bending durability of the embroidered receiver coil was evaluated using the custom bending rig shown in Fig. 11 that complies with international standard IPC-8981 [45]. A single receiver coil sample was mounted on the rig and subjected to repeated back-and-forth motion over a small 7.5 mm radius cylindrical rod, generating a 90-degree bending curve during each stroke with a tension of 2 N across the fabric. Electrical characterisation was performed at 0, 100 and 1000 bending cycles using the same VNA-based procedure described previously, with no retuning of the compensation network to ensure the measured PTE reflects the natural degradation of the coil under mechanical stress.

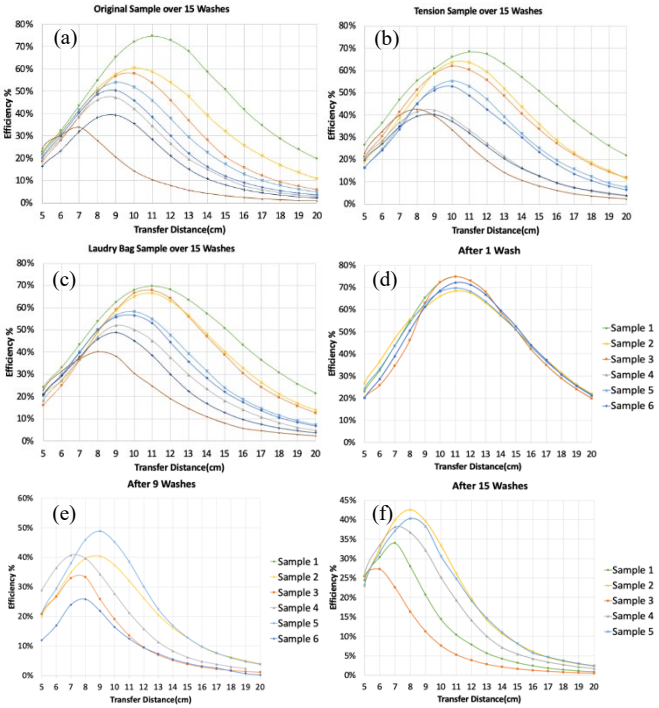

Fig. 10. PTE vs separation distance: (a) t-shirt sample 1 before and after various machine wash cycles. (b) T-shirt sample 2 with coil fabricated with increased stitching tension over 15 washes. (c) T-shirt sample 5 over 15 washed in a laundry bag. (d) All t-shirt samples after 1 wash. (e) All t-shirt samples after 9 washes. (f) All t-shirt samples after 15 washes.

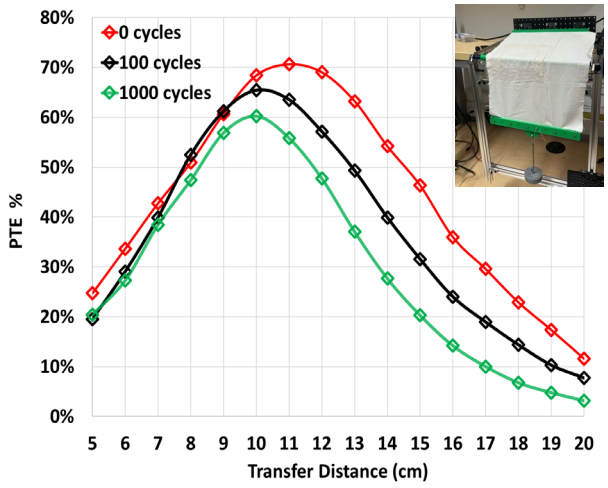

Fig. 11. PTE vs transfer distance after 0, 100 and 1000 bending cycles. Inset shows bending test rig with 2 N tension, stroke distance 15 cm, bending radius 7.5 mm

Fig. 11 presents the PTE measurements over different coil separation distances before bending and after 100 and 1000 cycles. The coil remained electrically functional after bending stages, but a progressive decline in PTE is observed, which correlates with the degradation in the coil's inductive performance, specifically the increase in AC resistance and reduction in inductance at the 6.78 MHz operating frequency. The Q-factor decreased from 143 at 0 cycles (L = 25.3 µH, Rac = 7.5 Ω) to 102 after 100 cycles (L = 23.2 µH, Rac = 9.6 Ω) and 81 after 1000 cycles (L = 21.0 µH, Rac = 11.2 Ω), corresponding to reductions of approximately 29% and 43%, respectively. This is due largely to the 50% increase in the coil resistance after 1000 cycles caused by the increase in resistance per unit length of the Litz wire aligned parallel to the movement direction. A moderate reduction in inductance was also observed, from 25.3 µH before bending to 21 µH after 1000 cycles (−17%), indicating that repeated high-curvature bending introduced small but measurable variations in the coil geometry. While these combined effects lead to reduced magnetic performance, the overall degradation remains moderate over 1000 cycles, demonstrating that the embroidered coil can tolerate routine bending stresses expected in wearable conditions.

F. Practical Charging

The ability of the textile-based MR-WPTs to transfer sufficient electrical power to an energy storage reservoir was evaluated by connecting the output to a capacitor after rectification. The separation distance was fixed at 15 cm, and the input power source was set at 20 dBm. Fig. 12a shows the voltage across a 1 mF electrolytic capacitor over 100 seconds. The 4-coil system achieves a significantly higher capacitor voltage of 2.66 V, equating to a stored energy of 3.55 mJ. The voltages achieved with the 2-coil MR-WPT and 3-coil MR-WPT after 100 seconds are 1.25 V and 1.6 V, respectively, equating to 0.79 mJ and 1.29 mJ, respectively. The capacitor voltage differed from the RMS voltage output in Fig. 5a due to the variation in load impedance. Charging a capacitor instead of a constant load introduces a varying and increased impedance mismatch, resulting in a loss of energy and a lower PTE.

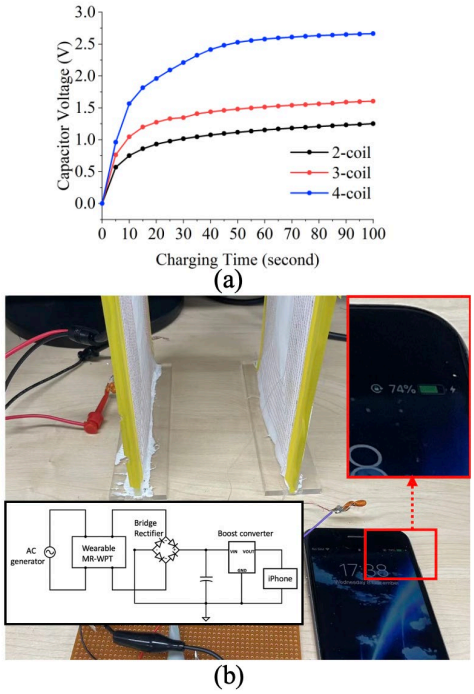

Fig. 12. (a) The charged capacitor voltage as a function of time for 1 mF electrolytic capacitor. (b) The textile-based MR-WPT charging an iPhone 6s.

Fig. 12b shows a different power management configuration for charging an iPhone 6s. The input power source was set as 24 dBm, and the transfer distance was 12 cm. The 3 and 4-coil systems took around 3 to 4 minutes to charge the iPhone from 70% to 71%, whilst the 2-coil system took over 5 minutes. Whilst it is not possible to calculate exact values for PTE and energy transferred, this does demonstrate the ability of the textile MR-WPT systems to power and recharge consumer electronics. While the delivered power (≈70–80 mW) is relatively low compared to conventional non-textile based mobile phone charging methods, it is certainly sufficient for typical low power e-textile systems for wearable applications and recharging small textile-based energy storage devices.

IV. Conclusion

The silk-coated, copper Litz wire coils couched onto a textile substrate form a flexible coil suitable for e-textile applications. The two-coil textile MR-WPT suffered the least impact from frequency splitting and had the shortest over-coupling region. In contrast, the 4-coil MR-WPT had the longest over-coupling region but achieved the maximum power transfer efficiency. The orientation studies showed that the MR-WPTs maintained at least 50% of the aligned performance before the coils were rotated beyond 40 degrees or axially misaligned by 6 cm for the two-coil system, and 60 degrees or axially misaligned by 8 cm for the 3 and 4-coil systems. Similarly, the four-coil structure was the least sensitive to bending up to 90 degrees. The 4-coil system maintained the highest PTE for coil misalignments and deformations that will typically occur in practical applications. The low Q-factor of the couched textile coils does limit the transmission range as a function of coil diameter compared with other coil types. Measures to increase the Q-factor, such as reducing the gap between turns and using a thicker, more densely packed, Litz wire with lower resistance per unit length, should be adopted. There will be a trade-off with respect to the feel of the textile, with such coils being more intrusive. The initial wash testing indicates that although the couching embroidery process with Litz wire produces the most effective textile coils for WPT, they are not sufficiently robust given the stitching parameters used in this study. There is also a reduction in PTE with repeated cyclical bending but this is due more to the change in resistance per unit length of the Litz wire. To improve coil robustness and minimize the reduction in PTE, the embroidery process needs further optimisation varying stitch the number of stitches per unit length or by double stitching the Litz wire. Otherwise, alternative ways of fabricating textile coils must be identified. Washing coils in a laundry bag is also a valid way of reducing the effects of machine washing.

References

[1] A. Komolafe et al., “Integrating Flexible Filament Circuits for E-Textile Applications,” Adv. Mater. Technol., vol. 4, no. 7, p. 1900176, July 2019.

[2] W. Zhou, L. Zhang, J. Zhang and S. Fu, “Textile Electrodes for Electrocardiogram Monitoring,” Adv. Mater. Technol., p. 2401279, 2024.

[3] S. W. Lee et al., “Bio-Inspired Electronic Textile Yarn-Based NO_2 Sensor Using Amyloid–Graphene Composite,” ACS Sens., vol. 6, no. 3, pp. 777–785, 2021.

[4] A. Komolafe et al., "E-Textile Technology Review–From Materials to Application," IEEE Access, vol. 9, pp. 97152-97179, 2021.

[5] M. Fernández, C. Vázquez and S. Ver Hoeye, "2.4 GHz Fully Woven Textile-Integrated Circularly Polarized Rectenna for Wireless Power Transfer Applications," IEEE Access, vol. 12, pp. 89836-89844, 2024.

[6] J. Kim, C. Cha, K. Lee, J. Oh and Y. Hong, "E-Textile-Based Wavy Surface WPT Flexible Antenna With Frequency Self-Reconfiguration Function for Batteryless Sensor Platform," IEEE Sens. J., vol. 23, no. 5, pp. 4392-4404, March 2023.

[7] M. Wagih, A. S. Weddell and S. Beeby, "Millimeter-Wave Textile Antenna for on-Body RF Energy Harvesting in Future 5G Networks," 2019 IEEE Wireless Power Transfer Conference (WPTC), London, UK, 2019, pp. 245-248.

[8] M. Wagih, N. Hillier, S. Yong, A. S. Weddell and S. Beeby, "RF-Powered Wearable Energy Harvesting and Storage Module Based on E-Textile Coplanar Waveguide Rectenna and Supercapacitor," IEEE Trans. Antennas Propag., vol. 2, pp. 302-314, 2021.

[9] D. Vital, J. L. Volakis and S. Bhardwaj, "A Wireless Power Transfer System (WPTS) Using Misalignment Resilient, On-Fabric Resonators for Wearable Applications," 2020 IEEE/MTT-S International Microwave Symposium (IMS), Los Angeles, CA, USA, 2020, pp. 1184-1187.

[10] E. Heo E, K.-Y. Choi, J. Kim, J.-H. Park and H. Lee, "A wearable textile antenna for wireless power transfer by magnetic resonance," Text. Res. J., vol. 88, no. 8, pp. 913-921, 2017.

[11] M. Wagih, A. Komolafe and B. Zaghari, "Dual-Receiver Wearable 6.78 MHz Resonant Inductive Wireless Power Transfer Glove Using Embroidered Textile Coils," IEEE Access, vol. 8, pp. 24630-24642, 2020.

[12] M. Wagih, A. Komolafe, I. Ullah, A. S. Weddell and S. Beeby, "A Wearable All-12Printed Textile-Based 6.78 MHz 15 W-Output Wireless Power Transfer System and Its Screen-Printed Joule Heater Application," IEEE Trans. Ind. Electron., vol. 71, no. 4, pp. 3741-3750, April 2024.

[13] S. Yong, J. Owen, and S. Beeby, “Solid-State Supercapacitor Fabricated in a Single Woven Textile Layer for E-Textiles Applications,” Adv. Eng. Mater., vol. 20, no. 5, p. 1700860, May 2018.

[14] Q. Xu, J. Chen, J. R. Loh, H. Zhong, K. Zhang, J. Xue, W. S. V. Lee, "Fiber-Shaped Batteries Towards High Performance and Perspectives of Corresponding Integrated Battery Textiles," Adv. Energy Mater., vol. 14, p. 2302536, 2024.

[15] X. Mou, D. T. Gladwin, R. Zhao, and H. Sun, “Survey on magnetic resonant coupling wireless power transfer technology for electric vehicle charging,” IET Power Electronics, vol. 12, no. 12, pp. 3005–3020, Oct. 2019.

[16] W. Zhong, C. K. Lee, and S. Y. R. Hui, “General Analysis on the Use of Tesla’s Resonators in Domino Forms for Wireless Power Transfer,” IEEE Trans. Ind. Electron., vol. 60, no. 1, pp. 261–270, Jan. 2013.

[17] D. W. Seo, “Comparative Analysis of Two- and Three-Coil WPT Systems Based on Transmission Efficiency,” IEEE Access, vol. 7, pp. 151962–151970, 2019.

[18] Z. Zhang, H. Pang, A. Georgiadis, and C. Cecati, “Wireless Power Transfer—An Overview,” IEEE Trans. Ind. Electron., vol. 66, no. 2, pp. 1044–1058, Feb. 2019.

[19] A. Kurs, A. Karalis, R. Moffatt, J. D. Joannopoulos, P. Fisher, and M. Soljačić, “Wireless Power Transfer via Strongly Coupled Magnetic Resonances,” Science, vol. 317, no. 5834, pp. 83–86, Jul. 2007.

[20] H. Hu and S. V. Georgakopoulos, “Multiband and Broadband Wireless Power Transfer Systems Using the Conformal Strongly Coupled Magnetic Resonance Method,” IEEE Trans. Ind. Electron., vol. 64, no. 5, pp. 3595–3607, May 2017.

[21] J.-G. Kim, G. Wei, M.-H. Kim, J.-Y. Jong, and C. Zhu, “A Comprehensive Study on Composite Resonant Circuit-Based Wireless Power Transfer Systems,” IEEE Trans. Ind. Electron., vol. 65, no. 6, pp. 4670–4680, Jun. 2018.

[22] S. Raju, R. Wu, M. Chan, and C. P. Yue, “Modeling of Mutual Coupling Between Planar Inductors in Wireless Power Applications,” IEEE Trans. Power Electron., vol. 29, no. 1, pp. 481–490, Jan. 2014.

[23] A. Karalis, J. D. Joannopoulos, and M. Soljačić, "Efficient wireless non-radiative mid-range energy transfer," Annals of Physics, vol. 323, no. 1, pp. 34–48, Jan. 2008.
[24] J. Zhang, X. Yuan, C. Wang, and Y. He, "Comparative Analysis of Two-Coil and Three-Coil Structures for Wireless Power Transfer," IEEE Trans. Power Electron., vol. 32, no. 1, pp. 341–352, Jan. 2017.
[25] Jian Zhang, Xinmei Yuan, and Chuang Wang, "A study of three-coil magnetically coupled resonators for wireless power transfer," in 2015 IEEE International Wireless Symposium (IWS 2015), Shenzhen, China, Mar. 2015, pp. 1–4.
[26] S. Moon, B.-C. Kim, S.-Y. Cho, and G.-W. Moon, "Analysis and design of wireless power transfer system with an intermediate coil for high efficiency," in 2013 IEEE ECCE Asia Downunder, Melbourne, Australia, Jun. 2013, pp. 1034–1040.
[27] T. P. Duong and J. -W. Lee, "Experimental Results of High-Efficiency Resonant Coupling Wireless Power Transfer Using a Variable Coupling Method," IEEE Microw. Wirel. Compon. Lett., vol. 21, no. 8, pp. 442-444, Aug. 2011.
[28] Y. Zhang, Z. Zhao, and K. Chen, "Frequency-Splitting Analysis of Four-Coil Resonant Wireless Power Transfer," IEEE Trans. on Ind. Applicat., vol. 50, no. 4, pp. 2436–2445, Jul. 2014.
[29] M. Rozman et al., "Combined Conformal Strongly-Coupled Magnetic Resonance for Efficient Wireless Power Transfer," Energies, vol. 10, no. 4, p. 498, Apr. 2017.
[30] D. Liu, H. Hu, and S. V. Georgakopoulos, "Misalignment Sensitivity of Strongly Coupled Wireless Power Transfer Systems," IEEE Trans. Power Electron., vol. 32, no. 7, pp. 5509–5519, Jul. 2017.
[31] K. Bao, C. L. Zekios, and S. V. Georgakopoulos, "A Wearable WPT System on Flexible Substrates," Antennas Wirel. Propag. Lett., vol. 18, no. 5, pp. 931–935, May 2019.
[32] S. Micus, L. Padani, M. Haupt, G.T. Gresser, "Textile-Based Coils for Inductive Wireless Power Transmission," Appl. Sci., vol. 11, p. 4309, 2021.
[33] N. Desai, J. Yoo and A. P. Chandrakasan, "A Scalable, 2.9 mW, 1 Mb/s e-Textiles Body Area Network Transceiver With Remotely-Powered Nodes and Bi-Directional Data Communication," IEEE J. Solid-State Circuits, vol. 49, no. 9, pp. 1995-2004, Sept. 2014
[34] N. J. Grabham, Y. Li, L. R. Clare, B. H. Stark, and S. P. Beeby, "Fabrication Techniques for Manufacturing Flexible Coils on Textiles for Inductive Power Transfer," IEEE Sens. J., vol. 18, no. 6, pp. 2599–2606, March 2018.
[35] M. R. Basar, M. Y. Ahmad, J. Cho, and F. Ibrahim, "An Improved Wearable Resonant Wireless Power Transfer System for Biomedical Capsule Endoscope," IEEE Trans. Ind. Electron., vol. 65, no. 10, pp. 7772-7781, 2018.
[36] S. Jeong et al., "Smartwatch Strap Wireless Power Transfer System with Flexible PCB Coil and Shielding Material," in IEEE Transactions on Industrial Electronics, vol. 66, no. 5, pp. 4054-4064.
[37] M. J. Jeong, T. Yun, J. J. Baek, and Y. T. Kim, "Wireless power transmission using a resonant coil consisting of conductive yarn for wearable devices," Text. Res. J., vol. 86, no. 14, pp. 1543–1548, 2016.
[38] T. Irshad, D. Ishak, and M. Baloch, "Comparative Analysis of Rectangular and Circular Four-resonator Coil System for Wireless Power Transfer Using Magnetic Resonance Coupling Technique," Eur. J. Electr. Eng., vol. 21, no. 1, pp. 67–73, Apr. 2019.
[39] Z. Luo and X. Wei, "Analysis of Square and Circular Planar Spiral Coils in Wireless Power Transfer System for Electric Vehicles," IEEE Trans. Ind. Electron., vol. 65, no. 1, pp. 331–341, Jan. 2018.
[40] A. P. Sample, D. A. Meyer, and J. R. Smith, "Analysis, Experimental Results, and Range Adaptation of Magnetically Coupled Resonators for Wireless Power Transfer," IEEE Trans. Ind. Electron., vol. 58, no. 2, pp. 544–554, Feb. 2011.
[41] Zhigang Dang and J. A. Abu Qahouq, "Range and misalignment tolerance comparisons between two-coil and four-coil wireless power transfer systems," in 2015 IEEE Applied Power Electronics Conference and Exposition (APEC), Charlotte, NC, USA, Mar. 2015, pp. 1234–1240.
[42] S. H. Kang, V. T. Nguyen, and C. W. Jung, "Analysis of MR-WPT using planar textile resonators for wearable applications," IET Microwaves, Antennas & Propagation, vol. 10, no. 14, pp. 1541–1546, Nov. 2016.
[43] Z. Dang and J. A. A. Qahouq, "Modeling and investigation of magnetic resonance coupled wireless power transfer system with lateral misalignment," in 2014 IEEE Applied Power Electronics Conference and Exposition - APEC 2014, Fort Worth, TX, USA, Mar. 2014, pp. 1317–1322.
[44] Y. Sun and S. Beeby, "Simulation of 2-Coil and 4-Coil Magnetic Resonance Wearable WPT Systems," in International Conference on the Challenges, Opportunities, Innovations and Applications in Electronic Textiles, Jan. 2021, p. 13.
[45] IPC-8981 "Quality and Reliability of E-Textiles Wearables", https://shop.electronics.org/ipc-8981/ipc-8981-standard-only

Yixuan Sun received the B.Eng. (with First Class Hons.) degree in electrical and electronic engineering in 2019 from the University of Southampton, Southampton, U.K., where she is currently working toward the Ph.D. degree in electronics and computer science.

Her research interests include magnetic resonant power transfer, wireless power transfer, flexible coils, and flexible circuits for wearable applications.

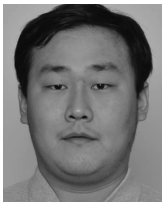

Sheng Yong received the Ph.D. degree in fabrication and characterization of fabric supercapacitors from the University of Southampton, U.K., in 2017.

He is currently a Research Fellow with the Centre for Flexible Electronics and E-Textiles, School of Electronics and Computer Science, University of Southampton. His current research interests include functional material formulation for e-textiles, and on developing energy storage devices for printed e-textiles, such as supercapacitors, primary and secondary batteries, and hybrid battery–supercapacitor energy storage devices.

Nick R. Harris received a BSc and MEng in Electronic and Electrical Engineering from the University of Bath in 1988 and 1989 respectively. He received his PhD from the University of Southampton in 1997.

He is a Professor in the School of Electronics and Computer Science Department, University of Southampton, Southampton, U.K., where he is involved in novel sensors and sensor systems, wireless sensor networks, microfluidic systems, ultrasonic particle manipulation, sonoporation and electroporation of cells, and energy harvesting, with funding from the EU, EPSRC, BBSRC, and industry. He is also a Chartered Engineer and a Co-Founder of Perpetuum Ltd. He has authored or coauthored more than 200 publications and patents in these fields. His research interests include sensors for rehabilitation systems, distributed sensors for agriculture and environmental monitoring, machine-learning approaches for distributed sensor systems, self-powered health and usage monitors, embedded condition-monitoring microsystems, ion-selective electrochemical sensors, and novel environmental energy harvesters.

Prof. Harris is a Member of the Institution of Engineering and Technology.

Stephen P. Beeby (Fellow, IEEE) received the B.Eng. (Hons.) degree in mechanical engineering from the University of Portsmouth in 1992 and the Ph.D. from the University of Southampton in 1998.

He is currently the Director of the Centre for Flexible Electronics and E-Textiles, University of Southampton. He is a cofounder of Perpetuum, Ltd., Smart Fabric Inks, Ltd., and D4 Technology, Ltd. His current research interests include energy harvesting, e-textiles, and the use of energy harvesting in wearable applications. He was the recipient of two EPSRC Research Fellowships to investigate the combination of screen-printed active materials with micromachined structures and textiles for energy harvesting. He has most recently been awarded a prestigious RAEng Chair in Emerging Technologies in E-textile Engineering.

Prof. Beeby is a Fellow of the Institute of Engineering and Technology, a Fellow of the Institute of Physics, a Chartered Engineer and a Chartered Physicist. Prof. Beeby won the 2025 IEEE Journal of Microwaves Best Paper Award with co-authors.